Proceedings of the ASME 2016 Dynamic Systems and Control Conference
DSCC 2016
October 12-14, 2016, Minneapolis, Minnesota, USA

DSCC2016-9907

DRAFT: DETECTION AND ANALYSIS OF COMBUSTION INSTABILITY FROM HI-SPEED FLAME IMAGES USING DYNAMIC MODE DECOMPOSITION

Sambuddha Ghosal[1,*], Vikram Ramanan[2], Soumalya Sarkar[3], Satyanarayanan R Chakravarthy[4] and Soumik Sarkar[5]

[1,5] Department of Mechanical Engineering, Iowa State University, Ames, IA
[2,4] Indian Institute of Technology Madras, Chennai, India
[3] United Technologies Research Center, East Hartford, CT

Emails: {[1]sghosal@iastate.edu, [2]vikrambest@yahoo.co.in, [3]sms388@gmail.com, [4]src@ae.iitm.ac.in, [5]soumiks@iastate.edu}

ABSTRACT

Flame dynamics and combustion instability is a complex problem involving different non-linearities. Combustion instability has several detrimental effects on flight-propulsion dynamics and structural integrity of gas turbines and any such spaces where combustion takes places internally, primarily in internal combustion engines. The description of coherent features of fluid flow in such cases is essential to our understanding of the flame dynamics and propagation processes. A method that is able to extract dynamic information from flow fields that are generated by a direct numerical simulation or visualized in a physical experiment (like in the case discussed in this paper) is Dynamic Mode Decomposition. This paper presents such a feature extraction and stability analysis of hi-speed combustion flames using Dynamic Mode Decomposition and it's sparsity promoting variant. Extensive experimental data was collected in a swirl-stabilized dump combustor at various operating conditions (e.g. premixing level and flow velocity) for analysing the flame stability conditions.

I. INTRODUCTION

In the present day, flame dynamics is an important topic of study owing to the complexities involved and also because of its immense applications. The non-linear and chaotic behaviour of flames and the physics associated with it arouses significant interest for many researchers. Flame dynamics is a result of coupling between turbulence, combustion and acoustics which lead to combustion instabilities. Such fluid flows are infinite dimensional systems governed by nonlinear partial differential equations. Even so, the essential features of their dynamical responses can be effectively approximated by models of lower complexity. These models utilize the concept of coherent structures. Coherent structures are organized fluid elements that, along with dynamic processes, are primarily responsible for most of the energy and momentum transfer in the flow. These structures are those whose generation mechanisms vary from system to system, and cause velocity oscillations and flame shape oscillations by curling and stretching. Of the more popular methods used for detecting these coherent structures are Proper Orthogonal Decomposition (POD) [1] and Dynamic Mode Decomposition (DMD) [2, 3], which utilises tools from spectral theory to derive spatial coherent structures. Application of POD and DMD on laminar flames has been shown in [4].

Dynamic Mode Decomposition is a relatively new technique proposed in [2]. It has been shown in [3] that DMD can be used to successfully analyse experimental data as well. It is based on Koopman Modes [5] and extracts data from snapshots associating a frequency to each mode. For combustion dynamics, frequency plays an important role and hence it is crucial that it is studied. Apart from the temporal frequency, the growth rate associated with a specific frequency can also be obtained from DMD analysis. Both POD and DMD are snapshot-based post-

*Address all correspondence to this author.

processing algorithms which may be applied equally well to data obtained in simulations or experiments. POD modes are characterized by spatial orthogonality and multi-frequential temporal content. DMD modes may be non-orthogonal with each of them possessing a single temporal frequency.

The basic idea behind using DMD is to construct the linear system matrix, that best explains the time-evolving data set of images. Spectral analysis of the said matrix helps us identify spatiotemporal coherent structures which are important from dynamical systems perspective. DMD is applied on specific zones approximated and pre-designated by another data-driven framework, "*Convolutional Neural Network* + *Symbolic Time Series Analysis*" ("$CNN + STSA$") [6] and thus also acts as a tool for its verification.

While DMD has been previously applied on PIV (Particle Image Velocimetry) data and laminar flame images, it is yet to be directly applied on time-varying complex flame images and extract coherent features from such images only. Also, techniques previously used to detect instability in such fluid flows such as *rms* variation of the pressure of the fluid prove insufficient in detecting said features. The work stated in this paper addresses this issue using DMD and its sparsity promoting variant, DMDSP (Sparsity Promoting Dynamic Mode Decomposition) [7] and studies how well it can determine the stability of a fluid flow from only its images captured at very high speeds which simplifies the instability detection procedure to a great extent.

To collect training data for determining flame stability conditions and learning coherent structures, thermo-acoustic instability was induced in a laboratory-scale combustor. The combustion images were captured using a hi-speed camera. The images captured for a particular flame-air flow mix conditions were then analysed using DMDSP by taking an optimal number of frames at every step by identifying five distinct zones of analysis predetermined by running the "$CNN + STSA$" framework.

II. PROBLEM FORMULATION AND EXPERIMENTAL SETUP

A. Problem Statement

Thermo-acoustic instability relates to the excitement of acoustics in a resonator with heat release rate fluctuations as the amplifier and source of such acoustics. The heat release rate fluctuations can be positively coupled to the pressure fluctuations through various mechanisms. Such mechanisms in general, are: 1. Velocity coupling and 2. Fuel concentration fluctuations. Velocity coupling is a broad term for different mechanisms, that involve both hydrodynamic and flame response to the former.

A prominent sustainer of combustion instabilities, especially in turbulent combustors is flame vortex interaction [2]. In fact, a number of studies on bluff body and rearward facing step combustors have highlighted in a qualitative manner (visual inspection) over a pressure cycle, the formation, evolution and interaction with flames [8, 9]. Reports in [10] have shown the onset of combustion instability as "lock-on" of the system acoustics to Karman vortex shedding mode, thus clearly marking such structures as the drivers of combustion instability. It must be noted that in any high *Re* (Reynold's Number) turbulent system, vortices of varying scales and intensity are present all the time, which however do not drive combustion instability. This is due to them not being coherent vortices as opposed to the vortices resulting from hydrodynamic instabilities. Coherent motions cause "in phase" or "uniform modulation" of the flames, thus causing large scale heat release rate fluctuations and consequently, combustion instability.

Detection of these coherent structures has been conventionally through visual inspection on flame images or through linear splitting techniques like POD [11]. The former is subjective and the latter though well tested, is applicable to only statistically stationary data. There are also concerns on POD modes being entirely physical in nature, although POD naturally identifies field data having high correlation values - a definitive property of coherent motion.

In the present work, we have attempted to characterize a turbulent swirl combustor for its thermo-acoustic properties by continuously varying a parameter (Re *or* Φ), (Φ is the equivalence ratio) thus operating from stable to unstable states. By virtue of the data being transient before having steady statistical values, application of the afore-mentioned mode extraction tool(s) is not possible. In order to estimate the growth and decay as well as possible exchange of energies between modes which are coherent, we apply Dynamic Mode Decomposition (DMD) [12] to analyse the transition data and find a suitable metric (defined in Section V) for the prediction of combustion instability. The metric is based on the lines of stability analysis and is seen to predict well the onset of combustion instability.

B. Experimental Setup and Description

The swirl combustor test bed used in this study has a swirler of diameter 30 mm with 60 degree vane angles, thus yielding a geometric swirl number of 1.28. Air to the combustor is fed through a settling chamber of diameter 280 mm with a sudden contraction leading to a square cross section of side 60 mm. This provides an area ratio of around 17, which thus acts as an acoustically open condition at the contraction. A mesh and honeycomb are mounted in immediate downstream of the contraction to provide uniform flow to the swirler. The combustor, shown in figure 1(a) consists of an inlet section of length 200 mm, an inlet optical access module (IOAM) of length 100 mm to provide optical access to the fuel tube, a primary combustion chamber of length 370 mm, and secondary duct of the same length. Extension ducts of the same cross section are added to provide length flexibility. The overall length of the constant area ducts was cho-

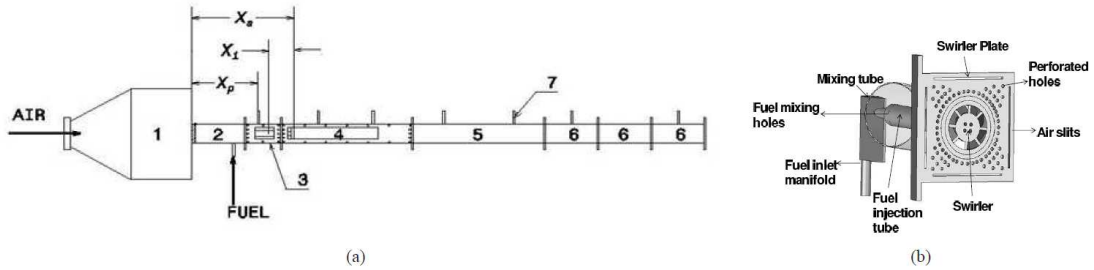

FIGURE 1. (a) Schematic of the experimental setup. 1 - settling chamber, 2 - inlet duct, 3 - IOAM, 4 - test section, 5 - big extension duct, 6 - small extension ducts, 7 - pressure transducers, X_s - swirler location measured downstream from settling chamber exit, X_p - transducer port location measured downstream from settling chamber exit, X_i - fuel injection location measured upstream from swirler exit, (b) Swirler assembly used in the combustor.

sen to be 1340 mm.

The fuel injection is done by injecting it coaxially with the air in a fuel injection tube with slots on the surface as shown in Figure 1(b). The fuel injection tube is coaxial to a mixing tube which has the same diameter as that of the swirler. The bypass air that does not enter the mixing tube passes through slots on the swirl plate. The slots on the fuel injection tube are drilled at designated distance upstream of the swirler. The larger this distance, more fuel mixes with the primary air in the mixing tube thus leading to more premixedness. Two upstream distances of $X_1 = 90mm$ and $X_2 = 120mm$ were chosen for this work. The upstream distance of 120 mm provides for full premixing of the fuel with the air. The 90 mm upstream injection case causes partial premixing of the fuel with air. The images were acquired at 3 kHz using Photron High speed star with a spatial resolution of 1024×1024 pixels.

Figure 2 presents sequences of images of dimension 392×1000 pixels for both stable ($Re = 7{,}971$, $FFR = 0.495g/s$ and full premixing) and unstable ($Re = 15{,}942$, $FFR = 0.495g/s$ and full premixing) states. The flame inlet is on the right side of each image and the flame flows downstream to the left. It can be observed that the flame does not have any prominent coherent structure when the combustion is stable. While the combustion is unstable, vortex shedding along the flow is observed. Bottom segment of the figure 2 shows formation of mushroom-shaped vortex at $t = 0, 0.001s$ and the shedding of that towards downstream from $t = 0.002s$ to $t = 0.004s$.

III. BRIEF BACKGROUND ON DMD AND DMDSP

A. Dynamic Mode Decomposition (DMD)

This section presents a brief background on DMD and DMDSP. For details refer to [2, 7]. DMD is a data processing technique that extracts coherent structures with a single temporal frequency from a numerical or experimental data-sequence. The primary steps of DMD and DMDSP are stated as follows:

The first step is to abstract a sequence of snapshots from a numerical simulation or physical experiments. In our case, physical experiments have been performed and these snapshots have been collected using a high-speed camera capturing the combustion flame images at *3kHz*. The next step is to form a data matrix whose columns represent the individual data samples. The data might need preprocessing to eliminate inherent noise. In this paper, although we deal with temporal evolution processes, it is noteworthy to mention that DMD can take into account a variety of other evolution processes and analyse them effectively. In our analysis of combustion flames, we assume that the image data are equispaced in time, with a time-step of say, Δt,

$$\left[\psi_0, \psi_1, ..., \psi_N\right]$$

,

where, in general, each $\psi_i := \psi(i\Delta t)$ is a complex vector with M measurement points (components), i.e., $\psi_i \in \mathbb{C}^M$. After this, we form from the snapshot sequence, two data matrices:

$$\Psi_0 := \left[\psi_0, \psi_1, ..., \psi_{N-1}\right] \in \mathbb{C}^{MXN},$$

$$\Psi_1 := \left[\psi_1, \psi_2, ..., \psi_N\right] \in \mathbb{C}^{MXN},$$

and propose a hypothesis that the snapshots were generated by a discrete-time time-invariant system which is governed by the relation:

$$\psi_{t+1} = A\psi_t, \quad t = 0, 1, ..., N-1. \tag{1}$$

Typically, in case of mass transfers (fluid flows), the matrix A contains a large number of entries which are complex numbers in general. DMD provides a procedure for determining a low-order representation of this matrix $A \in \mathbb{C}^{MXN}$ that captures the dynamics inherent in the flow data. In case of problems dealing with fluid flows, the number of measurement points (components) in each snapshot, ψ_i is typically much larger than the

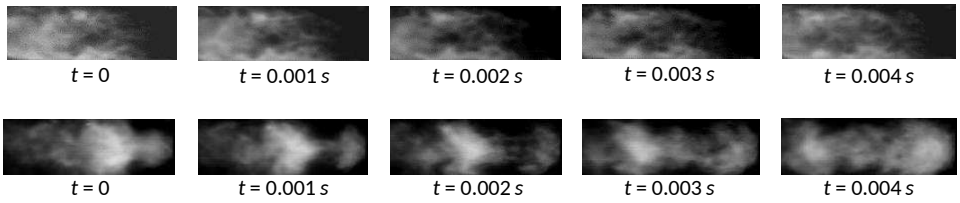

FIGURE 2. Combustion images used for flame stability analysis, captured at $3000\,fps\,(frames/second)$ *i.e.* $3kHz$; Top: greyscale images at $Re = 7,971$ and full premixing for a fuel flow rate of 0.495 g/s, bottom: greyscale images at $Re = 15,942$ and full premixing for a fuel flow rate of 0.495 g/s. *(Image Source: [13])*

number of snapshots themselves, i.e., $M \gg N$, implying that Ψ_0 and Ψ_1 are all tall matrices. Using the linear relation (1) between the snapshots at two consecutive time steps, the two data matrices Ψ_0 and Ψ_1 can be linked via the matrix A and Ψ_1 can be expressed as:

$$\Psi_1 = \left[\psi_1, \psi_2, ..., \psi_N\right] = \left[\mathrm{A}\psi_0, \mathrm{A}\psi_1, ..., \mathrm{A}\psi_{N-1}\right] = A\Psi_0 \quad (2)$$

Given a rank-r matrix of snapshots Ψ_0, the DMD algorithm provides us with an optimal representation $F \in \mathbb{C}^{r\times r}$ of the matrix A in the basis spanned by the POD modes of Ψ_0,

$$A \approx UFU^{\star}.$$

Here, $U^{\star}$ refers to the complex-conjugate-transpose of the matrix of POD modes of U which is obtained from an economy-size singular value decomposition (SVD) of $\psi_0 \in \mathbb{C}^{MXN}$ i.e.,

$$\Psi_0 = U\Sigma V^{\star},$$

where Σ is an $r \times r$ diagonal matrix with non-zero singular values $\sigma_1, ..., \sigma_r$ on its main diagonal, and

$$U \in \mathbb{C}^{M\times r} \; with \; U^{\star}U = I,$$

$$V \in \mathbb{C}^{r\times N} \; with \; V^{\star}V = I.$$

F can be determined from the matrices of snapshots Ψ_0 and Ψ_1 by minimizing the Frobenius norm of the difference between Ψ_1 and $A\Psi_0$ with $A = UFU^{\star}$ and $\Psi_0 = U\Sigma V^{\star}$,

$$\min_{F} \; \| \Psi_1 - UF\Sigma V^{\star} \|_F^2, \quad (3)$$

where the Frobenius norm of a given matrix, Q is can be obtained as follows:

$$\| Q \|_F^2 = trace(Q^{\star}Q) = trace(QQ^{\star}).$$

It is trivial to show that the optimal solution to (3) is given by

$$F_{dmd} = U^{\star}\Psi_1 V\Sigma^{-1}$$

which is identical to the expression provided in [2] and it implements the DMD algorithm, initializing from the two basic matrices of snapshots, Ψ_0 and Ψ_1. For further discussion on DMD, we refer to [2].

B. Determining the optimal amplitudes of DMD modes

The matrix $F_{dmd} \in \mathbb{C}^{r\times r}$ determines an optimal low-dimensional representation of $A \in \mathbb{C}^{M\times M}$ on the subspace spanned by the POD modes od Ψ_0. The dynamics on this r-dimensional subspace are governed by the equation:

$$x_{t+1} = F_{dmd}x_t \quad (4)$$

The matrix of POD modes U can be used to map x_t into a higher dimensional space $\mathbb{C}^M$ as,

$$\Psi_t \approx Ux_t.$$

The matrix, F_{dmd} can be brought into a diagonal coordinate form if it has a full set of linearly independent eigenvectors $\{y_1, ..., y_r\}$, with corresponding set of eigenvalues $\{\bar{\mu_1}, ..., \bar{\mu_r}\}$:

$$F_{dmd} = \underbrace{\begin{bmatrix} y_1 & \cdots & y_r \end{bmatrix}}_{Y} \underbrace{\begin{bmatrix} \mu_1 & & \\ & \ddots & \\ & & \mu_r \end{bmatrix}}_{D_\mu} \underbrace{\begin{bmatrix} z_1^{\star} \\ \vdots \\ z_r^{\star} \end{bmatrix}}_{Z^{\star}}$$

where, each y_j is of unit length, $y_j^\star y_j = 1$, and $\{z_1,...,z_r\}$ are the eigenvectors of $F_{dmd}^\star$, corresponding to the eigenvalues $\{\overline{\mu_1},...,\overline{\mu_r}\}$, scaled suitably to agree with the following bi-orthogonality condition:

$$z_i^\star y_j = \begin{cases} 1 \text{ if } i = j \\ 0 \text{ if } i \neq j. \end{cases}$$

The solution to (4) is now determined by -

$$x_t \;=\; Y D_\mu^t Z^\star x_0 \;=\; \sum_{i=1}^{r} y_i \mu_i^t z_i^\star x_0 \;=\; \sum_{i=1}^{r} y_i \mu_i^t \alpha_i,$$

Here $\alpha_i := z_i^\star x_0$ represents the *ith* modal contribution of the initial condition x_0. Thus, we can approximate experimental or numerical snapshots using a linear combination of the DMD modes, $\phi := U y_i$,

$$\psi_t \approx U x_t = \sum_{i=1}^{r} y_i \mu_i^t \alpha_i,\; t \in 0,...,N-1, \tag{5}$$

where each α_i can be interpreted as the "amplitude" of the corresponding DMD mode [2]. The selection of the amplitudes α_i can be interpreted as the selection of the Koopman modes that have the strongest influence on the system's response resulting from the use of the particular initial condition and the time interval on which the snapshots are collected. In matrix form,

$$\underbrace{\begin{bmatrix}\psi_0 & \psi_1 \cdots & \psi_{N-1}\end{bmatrix}}_{\Psi_0} \approx \underbrace{\begin{bmatrix}\phi_1 & \phi_2 \cdots & \phi_r\end{bmatrix}}_{\Phi} \underbrace{\begin{bmatrix}\alpha_1 & & & \\ & \alpha_2 & & \\ & & \ddots & \\ & & & \alpha_r\end{bmatrix}}_{D_\alpha := diag(\alpha)} \underbrace{\begin{bmatrix}1 & \mu_1 & \cdots & \mu_1^{N-1} \\ 1 & \mu_2 & \cdots & \mu_2^{N-1} \\ & \vdots & \vdots & \ddots \;\; \vdots \\ 1 & \mu_r & \cdots & \mu_r^{N-1}\end{bmatrix}}_{V_{and}},$$

The above expression demonstrates that the temporal evolution of the dynamic modes is governed by the Vandermonde matrix, $V_{and} \in \mathbb{C}^{r\times N}$. This matrix is determined by the r complex eigenvalues of μ_i of F_{dmd} which contain information about the underlying temporal frequencies and growth/decay rates. Determination of the unknown vector of amplitudes $\alpha := \begin{bmatrix}\alpha_1 \cdots \alpha_r\end{bmatrix}^T$ then boils down to finding the solution to the following optimization problem:

$$\min_{\alpha} \;\| \Psi_0 - \Phi D_\alpha V_{and} \|_F^2 \,.$$

which upon using the economy-size SVD of $\Psi_0 = U\Sigma V^\star$ and the definition of the matrix $\Phi := UY$, can be rewritten as:

$$\min_{\alpha} \; J(\alpha) := \| \Sigma V^\star - Y D_\alpha V_{and} \|_F^2, \tag{6}$$

This is a convex optimization problem that can be solved using standard methods as mentioned in [14]. We note that this optimization problem does access the POD modes of the matrix of snapshots Ψ_0; the problem data in (6) are the matrices Σ and V, which are obtained from the economy-size SVD of Ψ_0 and the matrices Y and V_{and}, which results from the eigenvalue decomposition of F_{dmd}. Thus, $J(\alpha)$ in (6) can be equivalently represented as

$$J(\alpha) \;=\; \alpha^\star P \alpha - q^\star \alpha - \alpha^\star q + s, \tag{7}$$

where

$$P := (Y^\star Y) \circ (\overline{V_{and} V_{and}^\star}),\; q := \overline{diag(V_{and} V \Sigma^\star Y)},\; s := trace(\Sigma^\star \Sigma).$$

The complex-conjugate-transpose of a matrix (vector) is denoted here by an asterisk. An overline denotes the complex-conjugate of a matrix (vector), "diag" of a vector is a diagonal matrix with its main diagonal determined by the elements of the vector, "diag" of a matrix is a vector determined by the main diagonal of the matrix, and $\circ$ is the elementwise multiplication of two matrices. The optimal vector of DMD amplitudes that solves the optimization problem (6) can therefore be obtained by minimizing the quadratic function (7) with respect to α,

$$\alpha_{dmd} = P^{-1} q = ((Y^\star Y) \circ (\overline{V_{and} V_{and}^\star}))^{-1} \overline{diag(V_{and} V \Sigma^\star Y)}.$$

Superposition of all DMD modes, properly weighted by their amplitudes and advanced in time according to their temporal growth/decay rate, optimally approximates the entire data sequence.

C. Sparsity-Promoting Dynamic Mode Decomposition (DMDSP)

In this paper, a modified form of DMD, its sparsity promoting variant, termed Sparsity Promoting Dynamic Mode Decomposition (DMDSP) has been used to define the instability measures defined in Section V. DMDSP is used to determine the performance of different number of frame sizes when compared to DMD and choosing the optimum frame size from the said analysis. It has also been used to develop and define a metric that gives us a measure of instability of the combustion flame dynamics that has been studied in this paper. DMDSP selects the

subset of DMD modes that has the most profound influence on the quality of approximation of a given sequence of snapshots. It provides a hierarchical description of the data sequence in terms of a set of dynamic modes. Further details and descriptions on DMDSP can be found in [7].

IV. RESULTS AND DISCUSSION

This section presents validation results and discussions along with pre-processing techniques applied on the snapshot sequence for applying DMDSP on it. For this study, the $600_{50\,to\,35}$ case is considered. The nomenclature refers to an air flow rate of 600 lpm (litres per minute) with fuel flow rate changing from an initial of 50 lpm to a final of 35 lpm.

First 7 seconds of the data for the given air and fuel flow rate is captured with the hi-speed camera. The image sequence taken for this time period is analyzed for its spectral content (integrated heat release rate) through Fast Fourier transform (FFT) over the entire duration to identify dominant frequencies present in the system. Although being transient in nature, the rise in amplitudes of the system at certain frequencies make FFT a convenient and easy choice to detect the same. We choose the optimum frame size for DMD analysis by detecting the dominant frequency (most amplified mode) by carrying out simple FFT on the data and observing the plot of the amplitude spectrum, as shown in Figure 3. It is observed to be $\approx 120.6\,Hz$, which corresponds to that of the duct natural mode of $120Hz$. DMD is performed on integral multiples of this duct mode time period with a minimum of five acoustic cycles [2] to start with. In this work, 25 images were grabbed per acoustic cycle, hence DMD is done on the snapshot sequence, whose length is varied starting from 150 (6 cycles) to 250 (10 cycles) frames in steps of 25 frames.

Within the image sequence, we obtain five zones based on analysis by the $CNN + STSA$ framework, which is further discussed in [6]. By means of Deep Learning which combines Conventional Neural network (CNN) with Symbolic Time Series Analysis (STSA) the method aims to extract coherent features from the transition data, by utilising pre-trained unstable flame images, thus aiming to predict combustion instability. It was observed that even before apparent transition to combustion instability, there were crests on the instability measure. These crests were labeled as intermittent regions for their non-monotonic behaviour. Two such intermittent regions were seen. Here, we primarily aim to identify the intermittent behaviour, through a DMD based metric. For this, DMD was performed on five regions - 1. Stable 2. First Intermittence 3. Second Intermittence 4. Transition and 5. Unstable based on operating conditions. These five zones are shown in Figure 4. The figure also shows the *rms* variation of pressure, which is one of the most commonly used measure of instability. It is to be noted that the pressure sensor by itself is unable to detect the instabilities.

Based on the aforementioned classification, we analyse the image sequence to choose the best frame size above 125 that ideally performs for the DMD and DMDSP algorithms. We choose multiples of 25 frames viz., 150, 175, 200, 225 and 250 frames to work on and determine frame sensitivity. We define a metric to determine the performance of DMDSP based on the number of frames chosen. The metric gives us, in percentage (%), how well DMDSP approximates the entire data sequence based on number of frames when evaluated across all the five designated zones under study. The plot is shown in Figure 4. With this figure as reference, the convergence behavior is evaluated by calculating the percentage reproduction of the initial snapshot of the image sequence from the summation of DMD eigenvectors calculated from the sparse DMD algorithm. The differences are then estimated by taking the difference of the Euclidean norm of the initial snapshot vector and the summed up eigenvectors. The results are plotted in Figure 5.

From Figure 5, it is clearly seen that there is little performance index change across the different snapshot length sequences. This establishes the fact that any frame size beyond 125 frames (starting from 150 in this case) will yield the same qualitative results, which will be independent of the number of frames. Since there is no preference for the number of frames, we perform DMDSP for each of these frame sizes and evaluate them based on the instability prediction performance. It is seen that 150 frames perform best overall with 79.73%, followed by 175 frames with 79.33%, 200 frames with 77.41%, 225 frames with 77.68% and 250 frames with 76.69%. We perform the sparse DMD algorithm by choosing 200 frames for the analysis, as the zones around which the analysis is carried out is approximated. We get a sound estimate of flame stability conditions for each of the five zones for the sequence of snapshots by choosing a window size of 200 frames. Performing this analysis, we define the flame instability measure which also verifies whether the defined metrics agree with the instability measure shown in Figure 4 and vice-versa.

Figure 6 shows the eigenvalues resulting from the standard DMD algorithm (black circles) along with the subset of N_z eigenvalues selected by the sparse DMD algorithm (red crosses) for the five different zones under consideration. Here, N_z represents the optimal number of sparse DMD modes. It is a well established fact that eigenvalues, when they lie outside the unit circle, depict unstable modes. When they lie inside the unit cirle, they are stable and when they lie on the unit circle itself, they are marginally stable.

A stability measure is thus defined from the information we get from Figure 6 regarding the position of the sparse DMD modes with respect to the unit circle. This metric is defined as the cumulative sum of the distances of each of the N_z DMDSP modes for each of the five zones, normalized over N_z. The instability measure defined by this metric is shown in Figure 8.

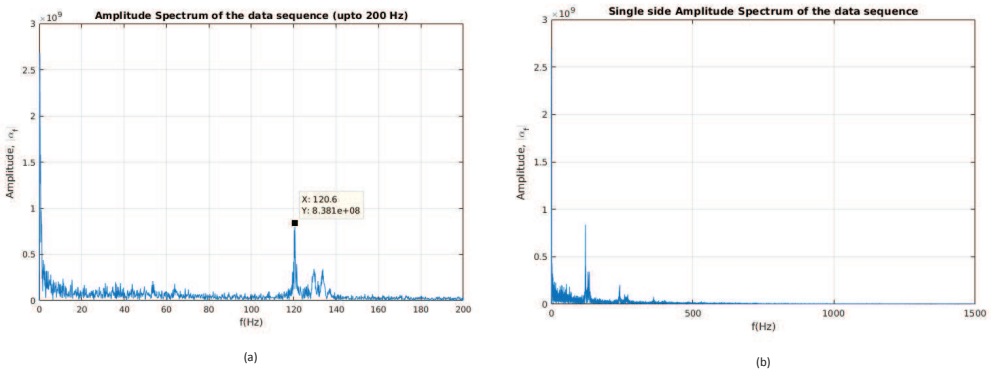

FIGURE 3. Fourier Analysis of the temporal image data to determine the dominant frequency: (a) Single side amplitude spectrum, plotted up to 200 Hz, showing the dominant frequency as $\approx 120.6\,Hz$, (b) Single side amplitude spectrum of the image data sequence (plotted up to half of the sampling frequency i.e. up to $1500\,Hz$

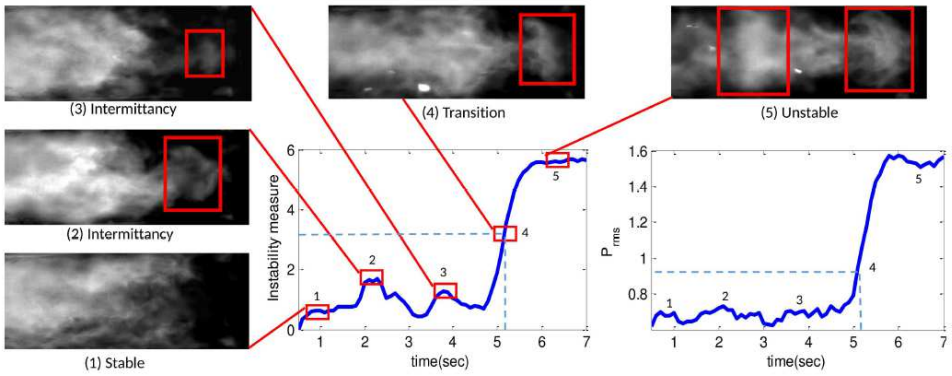

FIGURE 4. Variation of the proposed instability measure with time for the transition video named 600_{50to35}. Multiple regions on the measure curve denote different combustion states such as stable, temporary intermittency (a significant precursor to persistent instability) and unstable . They are corresponded to varied coherent structures (bounded by red box) that are detected by the CNN+STSA framework. On the right, *rms* variation of the pressure is shown as it is one of the most commonly used instability measures. Progression of P_{rms} can not detect the aforementioned precursors *(Image Source: [6])*

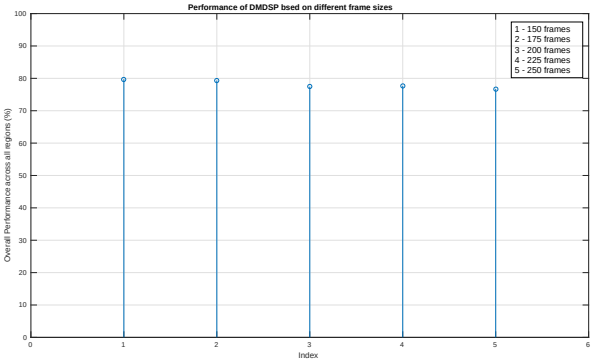

FIGURE 5. Performance of DMDSP subject to different frame sizes

The first Instability measure, M_1, is defined as:

$$M_1 = \sum_{i=1}^{N_z} (\delta_i)/N_z$$

where, δ_i is the distance of the individual DMDSP modes from the unit circle. The sum is normalized over the number of sparse DMD modes, N_z for each of the five zones. This normalization is done, as in case of the stable zone, $N_z = 27$ while for the other 4 zones, $N_z = 26$.

The stem-plot of M_1 for the different zones is shown in Figure 8. It gives us a broad idea of the flame stability conditions. We see that for the stable zone, the value of M_1 is the least, followed by the first intermittence zone, which has a slightly higher value than that of the stable zone, followed by second intermittence zone, which has a value ≈ 0. All of these three zones have negative values of M_1. Positive value of M_1 is shown only by the zones designated as "Transition" and "Unstable" by CNN+STSA. It is seen that the transition zone exhibits a higher value of M_1 than Unstable. This can be attributed to the frequent changes in flame behaviour with abrupt shedding and formation

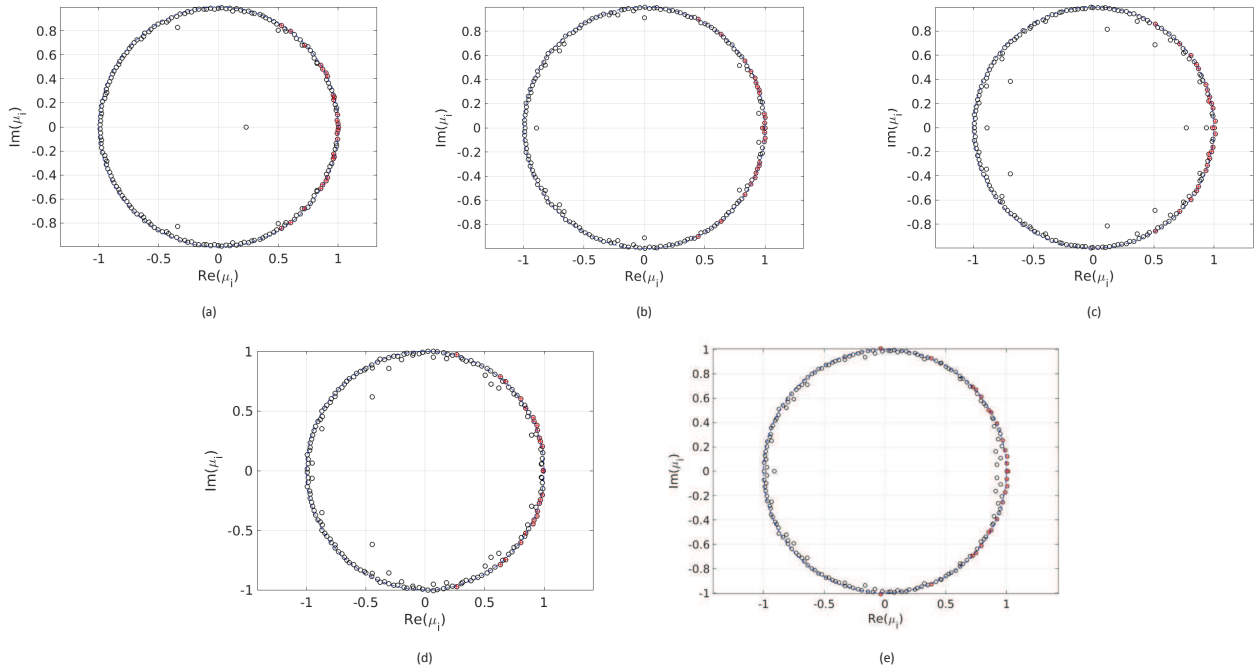

FIGURE 6. Eigenvalues resulting from the standard DMD algorithm (represented by black circles) along with the subset of N_z eigenvalues selected by the sparsity-promoting DMD algorithm (represented by red crosses) for (a) Stable Zone ($N_z = 27$), (b) First Intermittence Zone ($N_z = 26$), (c) Second Intermittence Zone ($N_z = 26$), (d) Transition Zone ($N_z = 26$) and (e) Unstable Zone ($N_z = 26$). The blue dashed curve identifies the unit circle.

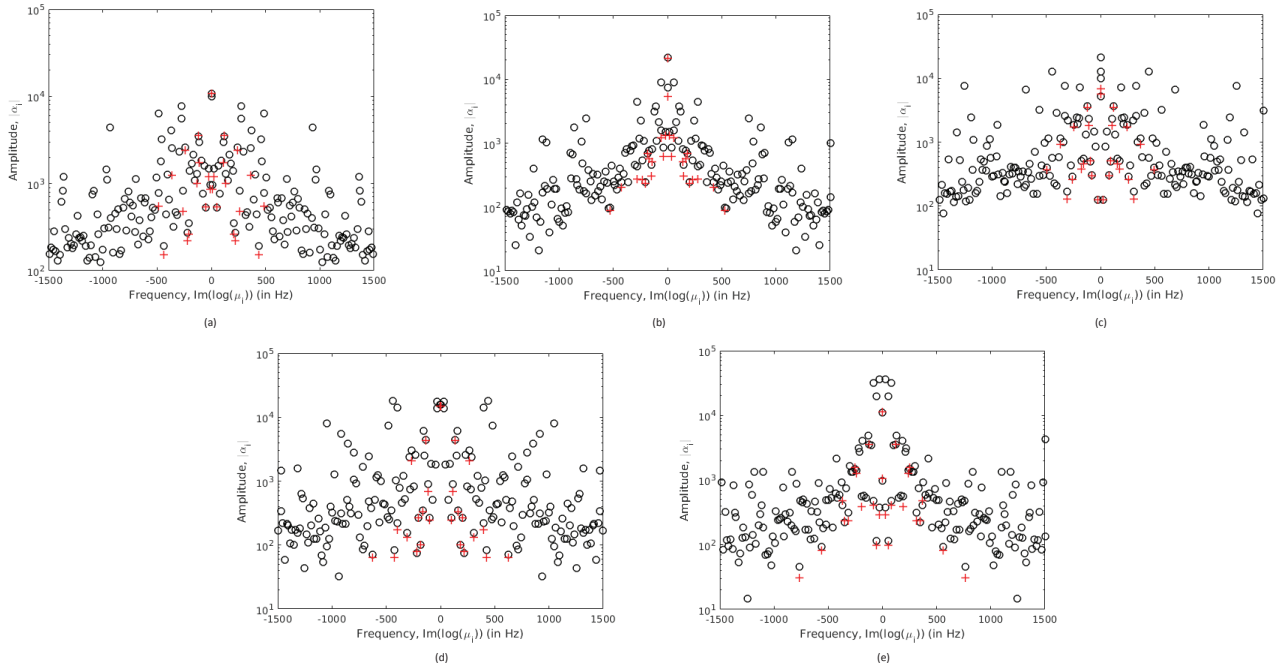

FIGURE 7. Dependence of the absolute value of the amplitudes α_i on the frequency (imaginary part) of the corresponding eigenvalues μ_i for (a) Stable Zone ($N_z = 27$), (b) First Intermittence Zone ($N_z = 26$), (c) Second Intermittence Zone ($N_z = 26$), (d) Transition Zone ($N_z = 26$) and (e) Unstable Zone ($N_z = 26$). The results are obtained using the standard DMD algorithm (black ircles) and the sparsity-promoting DMD algorithm (red crosses) with N_z DMD modes.

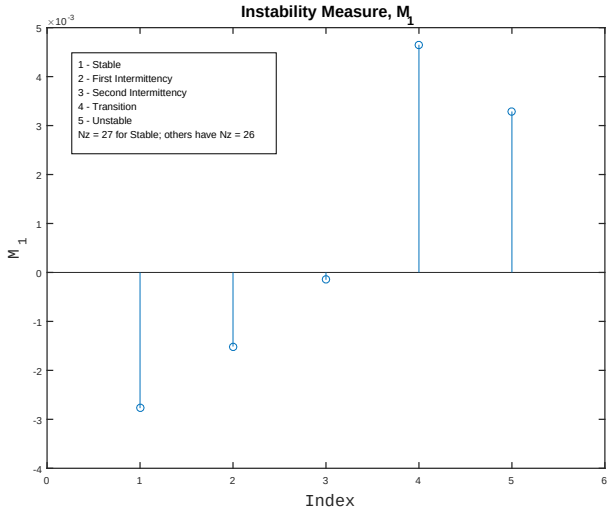

FIGURE 8. Variation of Instability measure, M_1 along the five zones under investigation

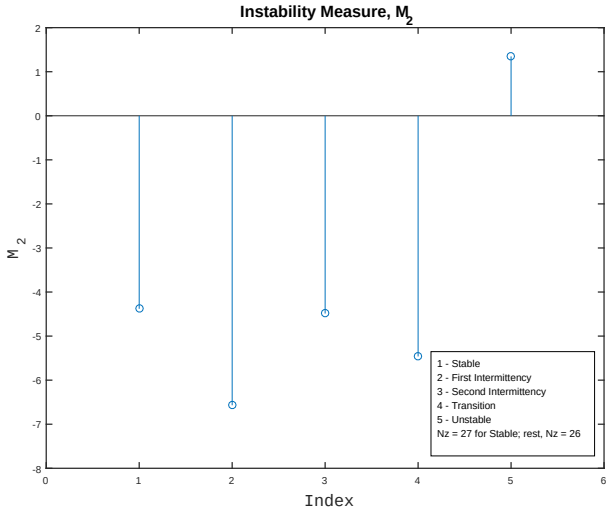

FIGURE 9. Variation of Instability measure, M_2 along the five zones under investigation

of intermittent vortices within the fluid flow that increases the value of the instability measure, registering a higher value of M_1 than the Unstable zone.

As discussed above, M_1 gives us a sense of stability for different zones in the fluid flow, by simply analysing the temporal image sequence by DMD and DMDSP. But, this analysis can only be attributed as a necessary but not a sufficient condition to detect stability. From Figure 8 alone, we cannot surely say whether a zone is stable or not. To get a better sense of the flame stability, the energy of each of these modes (determined by the amplitude of the modes) has tobe looked at. The amplitude vs frequency plot for the five zones are shown in Figure 7.

From Figure 7, we get the amplitudes (energies) corresponding to each of the modes (eigenvalues) determined in Figure 6. Knowing the weights of each of the sparse DMD modes, we now define a metric that gives us a sense of stability of the flame as it evolves with time. The metric is defined as the product of the distance to the unit circle of each of the DMDSP modes with the weight each of the mode carries with it. This gives more importance to the modes that represents and approximates the fluid flow to a greater extent than the modes whose weights are comparatively less. In defining this metric, the assumption is that the distance to the unit circle is considered as positive when the modes are outside of the unit circle and negative when the modes are inside the unit circle. The stability measure is given by the cumulative sum of this product for each of the modes (eigenvalues) obtained by running the DMDSP algorithm on the snapshot dataset for each of the five zones of investigation.

Now, we define our second instability measure, M_2 as:

$$M_2 = \sum_{i=1}^{N_z} (\delta_i \lambda_i)/N_z$$

where, δ_i is the same as defined before and λ_i is the amplitude (or energy or weight) of corresponding DMDSP mode.

Stability (or instability) measure of the flame for a specific zone, determined by the value of M_2 is shown in Figure 9.

As seen in Figure 9, the values of M_2 for stable, first and second intermittencies and transition zones are all negative. Only positive value of M_2 is exhibited by the unstable zone. This shows that, compared to the other four zones, true flame instability exists in only this region, when flame instability is most prominent, more so than the other zones which fail to exhibit when measured with respect to M_2. This is also verified from the experiment conditions where from it is noted that the conditions within the combustion chamber were tweaked to unstable conditions at the time instant when the flame instability was detected. This validates DMD and DMDSP as an effective analysis and verification tool for instability detection for combustion flames and also verifies the CNN+STSA approach proposed in [6].

V. SUMMARY, CONCLUSIONS AND FUTURE WORK

Pivoting on the spatio-temporal patterns exhibited by a turbulent combustor, and developed based on the sparse Dynamic Mode Decomposition algorithm, this paper proposes an effective analysis and verification tool that can be used for making online data-driven combustion instability detection techniques

such as CNN+STSA more accurate and robust by providing a solid physics-based understanding of combustion flame dynamics. The performance and prediction characteristics was carried out for varying number of frames and sparse DMD modes. The aforementioned analysis was done on five regions, with different dynamics as seen from a Convolutional Neural Network and Symbolic time series analysis approach.

Two metrics were devised based on the fundamental idea of the $l_2 - norm$ (spectral radius). It was seen that the instability measure for stable operations carries the most negative value compared to other selected regions as expected, indicating local stability. Furthermore, for the intermittent regions that were not seen to be either exhibiting stable or unstable behaviour from pressure data only, show negative values as well but these values registered higher than that for the stable zone, with the M_1 value for second intermittency being≈ 0. This implied that instability for the driving regions of the flame to excite acoustics in the flow were much more compared to the stable region but not enough $(still < 0)$ to transit to instability. Further, the transition region showed the highest positive value for M_1 compared to the other four regions, including the unstable region. This could be attributed to the fact that, at high pressure amplitudes (which corresponds to the unstable zone in this case), high levels of damping become significant and thus saturate the growth as well as reduce the instability measure.

DMD can be extended to extract spatial modes. These spatial modes, either at specific eigenvalues or to the full reconstruction can help in identifying changes in flame shape/ length and stabilization as the combustor approaches instability. Knowledge of this would eventually provide vital inputs to stability of flows and their instabilities that are critical in altering flame response and ultimately as the primary drivers of combustion instability.

Future work will include the development of a detection threshold that can be effectively used to detect label instabilities in not only combustion flames, but also in complex fluid flows. Furthermore, a challenge problem is to run the analysis at each and every step of the image data, by using a sliding window approach where we obtain the instability measures as a continuous variable instead of a discrete measure like the ones discussed here. The immediate next step is to visualise the data by reconstruction after identifying the most prominent coherent structures by detecting the sparse DMD modes which offer major contribution to the flow dynamics.

REFERENCES

[1] Berkooz, G., Holmes, P., and Lumley, J. L., 1993. "The proper orthogonal decomposition in the analysis of turbulent flows". *Annual review of fluid mechanics*, ***25***(1), pp. 539–575.

[2] Schmid, P. J., 2010. "Dynamic mode decomposition of numerical and experimental data". *Journal of Fluid Mechanics*, ***656***, pp. 5–28.

[3] Schmid, P. J., 2011. "Application of the dynamic mode decomposition to experimental data". *Experiments in Fluids*, ***50***(4), pp. 1123–1130.

[4] Chatterjee, S., Mukhopadhyay, A., and Sen, S., 2013. "Stability study of laminar flame using proper orthogonal decomposition and dynamic mode decomposition". *n3l - International Summer School and Workshop on Non-Normal and Nonlinear Effects in Aero- and Thermoacoustics, June 18-21, Munich*.

[5] Bagheri, S., 2013. "Koopman-mode decomposition of the cylinder wake". *J. Fluid Mech*, ***726***, pp. 596–623.

[6] Sarkar, S., Lore, K. G., and Sarkar, S., 2015. "Early detection of combustion instability by neural-symbolic analysis on hi-speed video". *NIPS 2015 workshop on Cognitive Computation: Integrating Neural and Symbolic Approaches, Montreal, Canada*.

[7] Jovanović, M. R., Schmid, P. J., and Nichols, J. W., 2014. "Sparsity-promoting dynamic mode decomposition". *Physics of Fluids (1994-present)*, ***26***(2), p. 024103.

[8] McManus, K., Poinsot, T., and Candel, S., 1993. "A review of active control of combustion instabilities". *Progress in energy and combustion science*, ***19***(1), pp. 1–29.

[9] Akintayo, A., Lore, K. G., Sarkar, S., and Sarkar, S., 2016. "Early detection of combustion instabilities using deep convolutional selective autoencoders on hi-speed flame video". *arXiv preprint arXiv:1603.07839*.

[10] Smith, D. A., and Zukoski, E. E., 1985. "Combustion instability sustained by unsteady vortex combustion". *American Institute of Aeronautics and Astronautics*.

[11] Candel, S., 2002. "Combustion dynamics and control: Progress and challenges". *Proceedings of the combustion institute*, ***29***(1), pp. 1–28.

[12] Chakravarthy, S. R., Shreenivasan, O. J., Boehm, B., Dreizler, A., and Janicka, J., 2007. "Experimental characterization of onset of acoustic instability in a nonpremixed half-dump combustor". *The Journal of the Acoustical Society of America*, ***122***(1), pp. 120–127.

[13] Sarkar, S., Lore, K. G., Sarkar, S., Ramanan, V., Chakravarthy, S. R., Phoha, S., and Ray, A., 2015. "Early detection of combustion instability from hi-speed flame images via deep learning and symbolic time series analysis". *Proceedings of Annual Conference of the Prognostics and Health Management Society, (San Diego, CA)*.

[14] Boyd, S., and Vandenberghe, L., 2004. *Convex optimization*. Cambridge University Press.